*R*esearch in
*A*stronomy and
*A*strophysics

Temporal variation of hemispheric solar rotation *

Jing-Lan Xie[1,2], Xiang-Jun Shi[1,2] and Jing-Chen Xu[1,2]

[1] National Astronomical Observatories / Yunnan Observatory, Chinese Academy of Sciences, Kunming 650011, China; *xiejinglan@ynao.ac.cn*
[2] Graduate University of Chinese Academy of Sciences, Beijing 100049, China

Abstract The daily sunspot numbers of the whole disk as well as the northern and southern hemispheres from 1945 January 1 to 2010 December 31 are used to investigate the temporal variation of rotational cycle length through the continuous wavelet transformation analysis method. Auto-correlation function analysis of daily hemispheric sunspot numbers shows that the southern hemisphere rotates faster than the northern hemisphere. The results obtained from the wavelet transformation analysis are that no direct relationship exists between the variation trend of the rotational cycle length and the solar activity in the two hemispheres and that the rotational cycle length of both hemispheres has no significant period appearing at 11 yr, but has a significant period of about 7.6 yr. Analysis concerning the solar cycle dependence of the rotational cycle length shows that acceleration seems to appear before the minimum time of solar activity in the whole disk and the northern hemisphere, respectively. Furthermore, the cross-correlation study indicates that the rotational cycle length of the two hemispheres has different phases, and that the rotational cycle length of the whole disk as well as the northern and southern hemispheres, also has phase shifts with corresponding solar activity. In addition, the temporal variation of the north-south (N-S) asymmetry of the rotational cycle length is also studied. This displays the same variation trend as the N-S asymmetry of solar activity in a solar cycle, as well as in the considered time interval, and has two significant periods of 7.7 and 17.5 yr. Moreover, the rotational cycle length and the N-S asymmetry of solar activity are highly correlated. It is inferred that the northern hemisphere should rotate faster at the beginning of solar cycle 24.

Key words: Sun: activity — Sun: rotation — Sun: sunspot

1 INTRODUCTION

There are two main methods used in investigating the solar rotation rate: the trace method and the spectroscopic method (Paternò 2010). It is found that the Sun has a higher rotation rate in the equatorial region: 26 d at the equator and 30 d at $60°$ latitude (Lawrence et al. 2008; Le Mouël et al. 2007). More details about different measures of the Sun's rotation rate can be found in the review papers (Howard 1984; Schroeter 1985; Snodgrass 1992; Beck 2000; Paternò 2010). In hoping to reach a

more synthetic view of solar rotation, Heristchi & Mouradian (2009) suggested a method called global rotation that was applied to structures of solar activity. Using this method, they indicated that individual structures, local proper motions, meridian drift or differential rotation could be analyzed together in the considered time.

How solar differential rotation varies in a solar cycle, as well as over a long period, is still an unsolved problem. Li et al. (2011a,b) used a continuous complex Morlet wavelet transformation to investigate the temporal variations of the rotational cycle length of daily sunspot areas and sunspot numbers from a global point of view, and indicated that the rotational cycle length of the Sun had a secular trend and that the rotational period had no relation with the Schwabe cycle. Li et al. (2011b) pointed out that a lower than average rotation velocity should statistically appear around the maximum time of solar activity, while around the minimum time the rotation velocity was very close to the average. However, Gilman & Howard (1984), Zuccarello & Zappalá (2003) and Brajša et al. (2006) claimed that a higher than average rotation velocity appears in the minimum time of solar activity.

North-south (N-S) asymmetry in solar activity is an important part of solar physics. A lot of research has been done based on various solar activity indices on the solar surface. More details about N-S asymmetry can be found in Vizoso & Ballester (1990), Verma (1993), Carbonell et al. (1993, 2007), Li et al. (2001, 2002, 2010) and Sýkora & Rybák (2010). Besides, rotational periods are also subjected to an N-S asymmetry (Temmer et al. 2003). Gilman & Howard (1984) found that in the northern hemisphere rotation is more solid-body-like. Javaraiah & Ulrich (2006) indicated that differences exist in the hemispheric rotation rates. Howard et al. (1984) analyzed the large spot data and found that the rotation rate increases less in the northern hemisphere. Antonucci et al. (1990) investigated the rotational period of the photospheric magnetic field during cycle 21 and their results showed that the two hemispheres have different dominant periods: 26.9 d for the northern hemisphere and 28.1 d for the southern hemisphere. Also, the results of Temmer et al. (2002a,b) concerning the rotational periods of Hα flare and sunspot numbers accorded with the periods found by Antonucci et al. (1990). However, the observational results of Balthasar et al. (1986) indicated that sunspots have a slightly higher rotation rate in the southern hemisphere, and this was discovered by analyzing sunspot groups of all types in the period 1874–1976. Georgieva & Kirov (2003) indicated that the two hemispheres not only rotate differently but also have different periodicities in the variations of the rotation parameters. The N-S asymmetry in hydrogen filament rotation has been studied by Gigolashvili (2001) and Gigolashvili et al. (2003). They found that the sign of asymmetry changes with the hale period, and they suggested that the N-S asymmetry of solar rotation might be connected with the N-S asymmetry of solar activity.

This work follows the previous study of Li et al. (2011a,b). We still use the continuous complex Morlet wavelet transformation to obtain the rotational signals reflected in the daily hemispheric sunspots' wavelet power spectrum from a global point of view, and then conduct further research on the temporal variation of solar rotation separately in the northern and southern hemispheres and on their relationship with hemispheric solar activity. In addition, we investigate the N-S asymmetry of the solar rotational cycle length, including its time-variation, periodicity, and relationship with the N-S asymmetry of solar activity.

2 THE ROTATIONAL SIGNAL IN DAILY HEMISPHERIC SUNSPOT NUMBERS

2.1 Data

The time series data analyzed in our study are the following.

(1) The daily northern and southern hemispheric sunspot numbers (1945 January 1 to 2004 December 31)[1], compiled by Temmer et al. (2006).

---

[1] *ftp://cdsarc.u-strasbg.fr/pub/cats/J/A+A/447/735/*

(2) The daily northern and southern hemispheric international sunspot numbers (2005 January 1
    to 2010 December 31)[2]. This time series actually starts from 1992 January 1, thus there is an
    overlapping time span from 1992 January 1 through 2004 December 31 with the first time series.
    However, in general, the first one renders the second very well (for details see Temmer et al.
    2006).

Figure 1 shows the data and their linear regressions against time (the daily sunspot number on
the whole solar disk at a certain time is the number in the northern hemisphere plus that in the south
at the same time). It is obvious that the daily sunspot numbers of the whole solar disk, as well as the
northern and southern hemispheres all have a decreasing trend during the time interval considered.
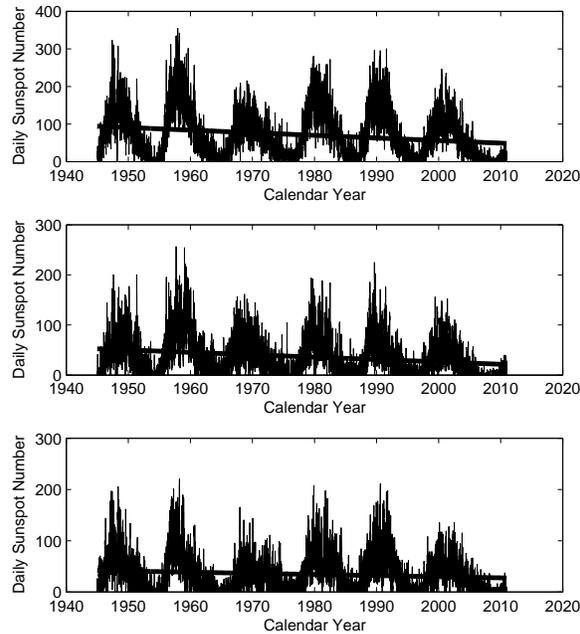
Fig. 1 Daily sunspot numbers of the whole disk (*top panel*), the northern hemisphere (*middle panel*),
and the southern hemisphere (*bottom panel*) from 1945 January 1 to 2010 December 31. The thick
solid lines are their corresponding linear regression lines.

2.2 Rotational Period

The auto-correlation function is used here to detect the periodicity of daily hemispheric sunspot
numbers, which is shown in Figure 2. The auto-correlation coefficients of the daily hemispheric
sunspot numbers show that the rotational period is the only period within a time scale shorter than
1 yr, whose value is 26, 27 and 26 d for the whole disk, the northern and the southern hemispheres,
respectively. This means that the southern hemisphere rotates faster over the considered time interval.
We also employ the continuous complex Morlet (dimensionless frequency $\omega_0 = 6$) wavelet
transformation (Torrence & Compo 1998) here to study the periodicity of daily hemispheric sunspot

---

[2] *http://sidc.oma.be/sunspot-data/*
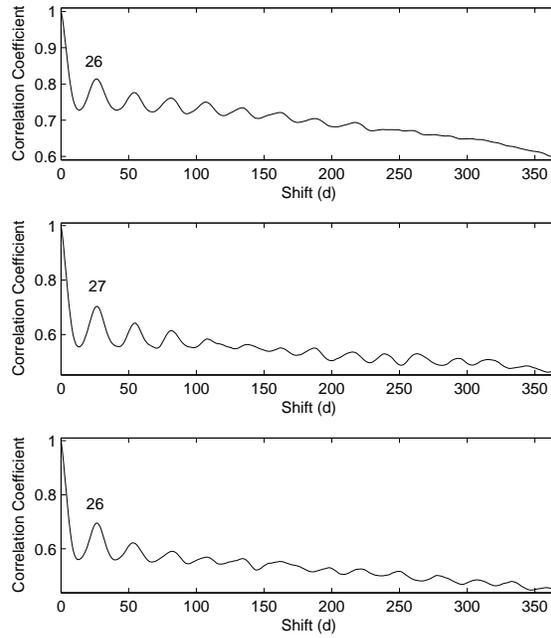
Fig. 2 Auto-correlation function of the daily hemispheric sunspot numbers for the period from 1945 January 1 to 2010 December 31, plotted up to a time lag of 365 d. The *top panel* is for the whole disk, the *middle panel* the northern hemisphere, and the *bottom panel* the southern hemisphere.

numbers. The wavelet analysis decomposes a transform from a one-dimensional time series into a two-dimensional time-frequency space. Therefore, this method determines not only the periodicities of the dominant modes of variability, but also shows how the modes vary in time (Torrence & Compo 1998; Chowdhury & Dwivedi 2011). The Morlet wavelet used in the paper is defined as

$$\Psi_0(\eta) = \pi^{-1/4}e^{i\omega_0\eta}e^{-\eta^2/2}\,,\tag{1}$$

where ω_0 is the dimensionless frequency and η is the dimensionless time. When using wavelets for feature-extraction purposes, the Morlet wavelet (with $\omega_0 = 6$) is a good choice, since it provides a good balance between time and frequency localization (Torrence & Compo 1998; Grinsted et al. 2004).

As the wavelet is not completely localized in time, the continuous wavelet transformation is subject to edge artifacts. It is thus useful to introduce a cone of influence (COI) in which the transform suffers from these edge effects. COI is defined as the wavelet power for a discontinuity at the edges which decreases by a factor of e^{-2}. Portions of the transform that are outside the area encompassed by the time axis and the COI are subject to these edge effects and are therefore unreliable (Torrence & Compo 1998; Grinsted et al. 2004; De Moortel et al. 2004; Li et al. 2006; Chowdhury & Dwivedi 2011).

The significance levels for the wavelet power spectra are calculated assuming a mean background spectrum modelled with a univariate lag-1 autoregressive process. To determine the significance levels, one first needs to choose an appropriate background spectrum. For many time series, an appropriate background spectrum is either white noise or red noise. Throughout this paper, the statistical significance test is carried out by assuming that the noise has a red spectrum, that is a red
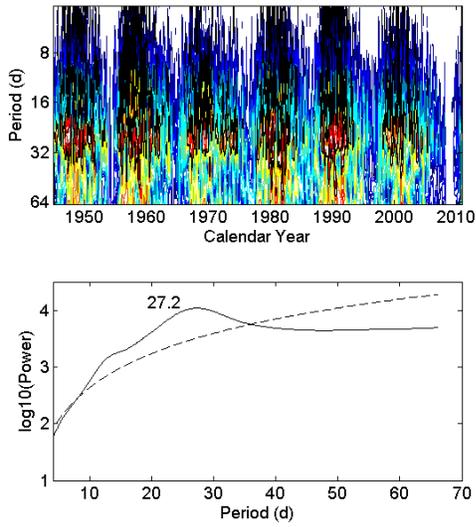
Fig. 3 *Top panel*: the continuous wavelet power spectrum of the daily sunspot numbers; *bottom panel*: the global power spectrum (*solid line*) of daily sunspot numbers. The *dashed line* shows the 95% confidence level.
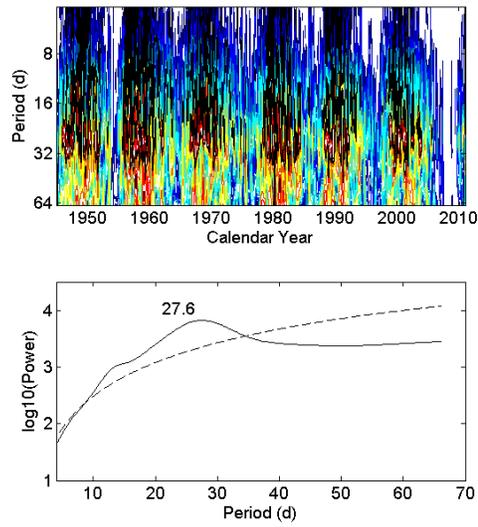
Fig. 4 *Top panel*: the continuous wavelet power spectrum of the daily northern sunspot numbers; *bottom panel*: the global power spectrum (*solid line*) of daily northern sunspot numbers. The *dashed line* shows the 95% confidence level.
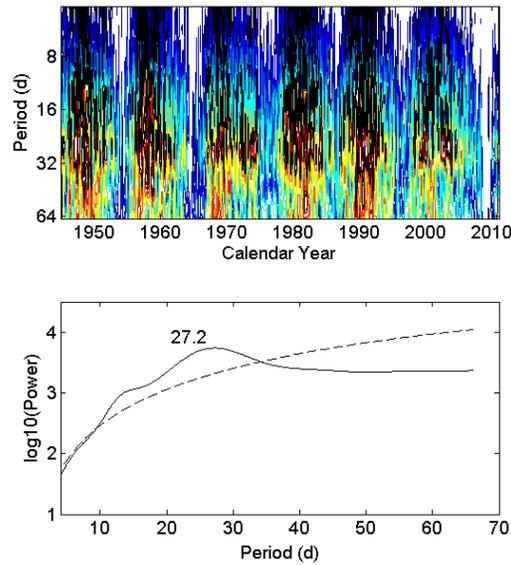
Fig. 5 *Top panel*: the continuous wavelet power spectrum of the daily southern sunspot numbers; *bottom panel*: the global power spectrum (*solid line*) of daily southern sunspot numbers. The *dashed line* shows the 95% confidence level.

noise background is considered. In a red noise spectrum, the discrete Fourier power spectrum, after normalizing, is

$$P_k = \frac{1 - \alpha^2}{1 + \alpha^2 - 2\alpha \cos(2\pi k/N)} \,, \tag{2}$$

where $k = 0, \ldots, N/2$ is the frequency index, N is the data number and α is the assumed lag-1 autocorrelation. When $\alpha = 0$, we obtain the white-noise spectrum with an expectation value of one at all frequencies (Torrence & Compo 1998; Chowdhury & Dwivedi 2011).

Presented in Figures 3 to 5 are the local wavelet power spectrum and the global power spectrum of the daily sunspot numbers for the whole disk, the northern hemisphere and the southern hemisphere, respectively. Before performing the wavelet transformation, the raw data need to be normalized, that is the process of subtracting the mean value of the data and then dividing it by the variance of the data. As the local wavelet power spectrum shows, the highest power belt appears around the rotational cycle of the Sun, and this can be seen clearly around the maximum time of the sunspot cycle. The global power spectrum figures also indicate that the rotation period is the only period (at the 95% confidence level), in the time scale shorter than 64 d. From a global point of view, the values of the rotational periods are 27.2, 27.6, and 27.2 d for the whole disk, the northern and the southern hemispheres, respectively.

2.3 Long-Term Variations of the Solar Rotation

How the period length of the rotational cycle (PLRC) changes with time is presented in Figure 6. At a certain time point, the rotational period (scale) has the highest spectral power among the period scales from 25 to 31 d (the cycle length of the differential rotation of sunspots is also located within this range (Temmer et al. 2002b; Yin et al. 2007) in the local wavelet power spectrum (see Figs. 3 to 5), and using that the rotational period at each time can be determined. Next, a two-year smoothing was introduced to the obtained temporal variation of the rotational cycle length, and the new time series and linear regression lines are given in Figure 6. The rotational cycle length of the northern and southern hemispheres has different varying trends, but as Figure 1 shows, the hemispheric sunspot numbers have the same decreasing trends. Hence, we suggest that the trend of the rotation rate possibly has no direct relation with the trend of the sunspot numbers.

Moreover, as Brajša et al. (2006) and Li et al. (2011b) did, we also investigate the cycle-related variation of the solar rotation rate, separated into the whole disk, the northern and the southern hemispheres, respectively. As Figure 7 shows, in the whole disk and the northern hemisphere, a higher than average velocity appears before the minimum time of solar activity. However, in the southern hemisphere, the pattern is not clearly seen. Maybe it is affected by the phase difference between the northern and southern hemispheres (see Sect. 3).

2.4 The Periodicity in the Temporal PLRC

For further study, the complex Morlet (dimensionless frequency $\omega_0 = 6$) wavelet transformation (Torrence & Compo 1998) is again used to investigate the periodicity in the temporal PLRC of daily hemispheric sunspot numbers, and the results are shown in Figures 8 to 10. PLRC is normalized first too. For PLRC, no significant period (scale) seems to appear at the 11 yr Schwabe cycle in the whole disk as well as in the northern and southern hemispheres. This indicates that PLRC might have no relation with the Schwabe cycle, which is in agreement with Li et al. (2011a). However, two significant periods of 7.7 and 19.5 yr can be seen for the northern hemisphere, while 4.7, 7.6, 17.2 and 25.1 yr can be seen for the southern hemisphere and 4.8 and 23.1 yr for the whole disk (since the data are smoothed over 2 yr, periods less than 2 yr are not reliable).
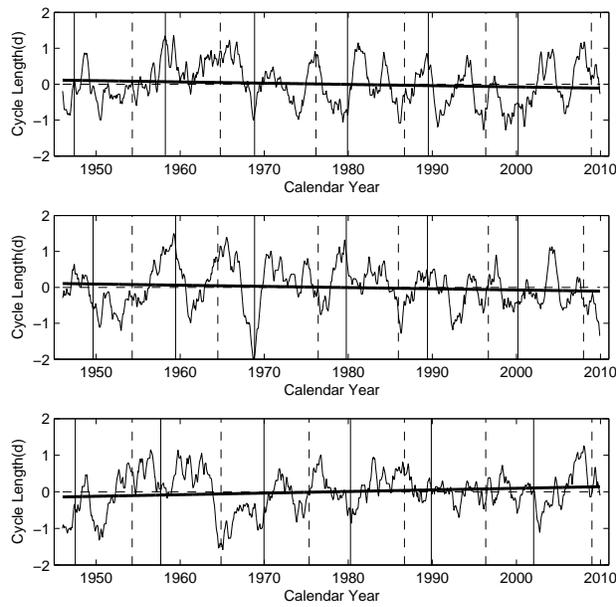
Fig. 6 The period length (*thin lines*) of the rotational cycle of daily sunspot numbers relative to the mean cycle length. The thick solid lines show their secular trends. The vertical solid (*dashed*) lines indicate the maximum (minimum) times of sunspot cycles. The three panels are, from top to bottom, for the whole disk, the northern hemisphere and the southern hemisphere, respectively.
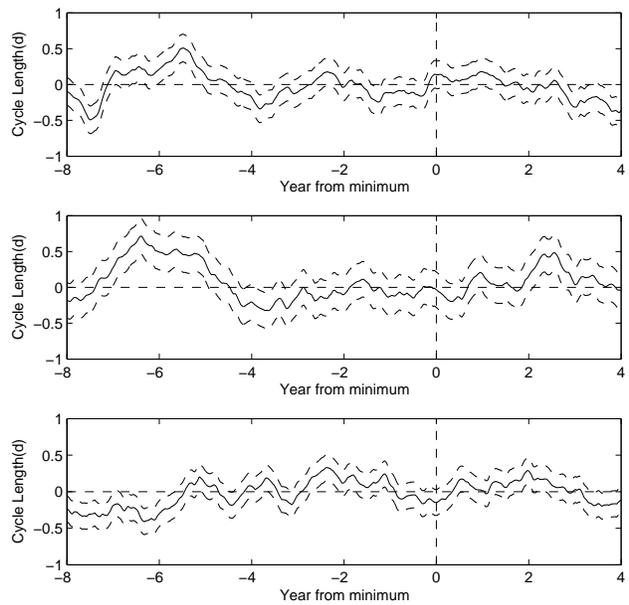
Fig. 7 Dependence of the period length (*solid lines*) of the rotational cycle (relative to mean cycle length) on the phase of the solar cycle, with respect to the nearest preceding sunspot minimum. The dashed lines show their corresponding standard errors. The three panels are, from top to bottom, for the whole disk, the northern hemisphere and the southern hemisphere, respectively.
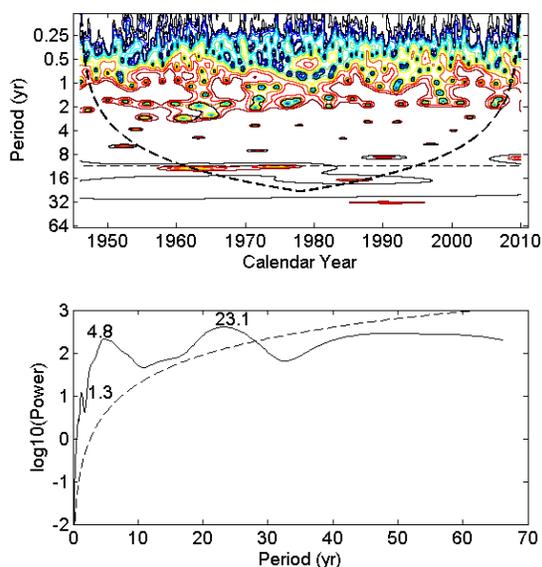
Fig. 8 *Top panel:* the continuous wavelet power spectrum of the period length of the rotational cycle of the daily sunspot numbers. The black solid contours indicate the 95% confidence level. The region below the thick dashed line indicates the COI where edge effects might distort the picture (Torrence & Compo 1998). The horizontal dashed line stands for the scale of 11.0 yr. *Bottom panel*: the global power spectrum (*solid line*) of the period length of the rotational cycle of daily sunspot numbers. The dashed line shows the 95% confidence level.
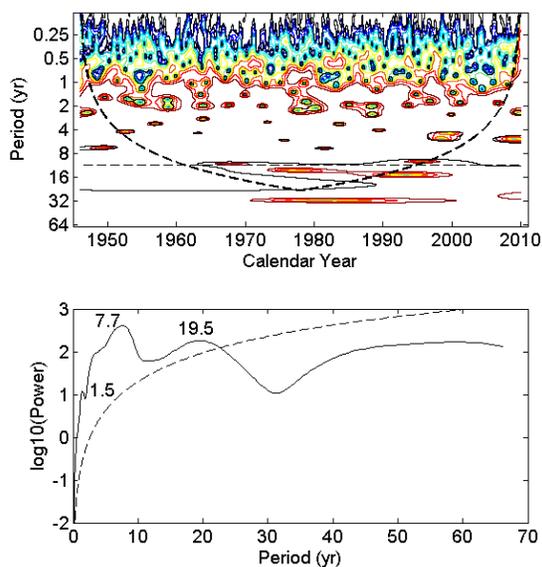
Fig. 9 *Top panel*: the continuous wavelet power spectrum of the period length of the rotational cycle of the daily northern sunspot numbers. The black solid contours indicate the 95% confidence level. The region below the thick dashed line indicates the COI where edge effects might distort the picture (Torrence & Compo 1998). The horizontal dashed line stands for the scale of 11.0 yr. *Bottom panel*: the global power spectrum (*solid line*) of the period length of the rotational cycle of daily northern sunspot numbers. The dashed line shows the 95% confidence level.
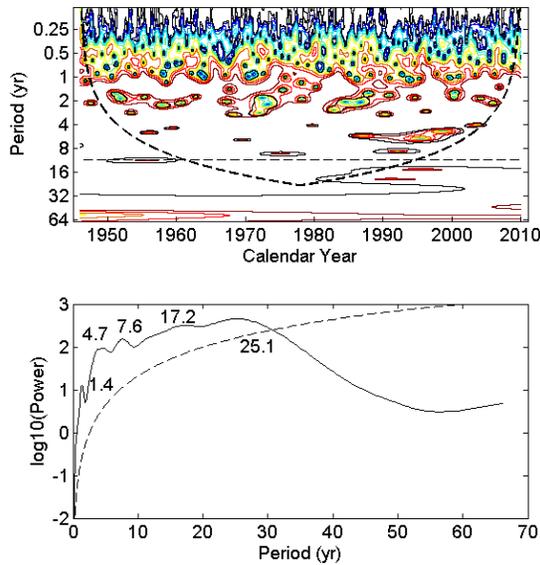
Fig. 10 *Top panel:* the continuous wavelet power spectrum of the period length of the rotational cycle of the daily southern sunspot numbers. The black solid contours indicate the 95% confidence level. The region below the thick dashed line indicates the COI where edge effects might distort the picture (Torrence & Compo 1998). The horizontal dashed line stands for the scale of 11.0 yr. *Bottom panel:* the global power spectrum (*solid line*) of the period length of the rotational cycle of daily southern sunspot numbers. The dashed line shows the 95% confidence level.

3 RELATIONSHIP OF PLRC WITH SOLAR ACTIVITY

Figure 11 shows the cross-correlation coefficient between the smoothed rotational cycle length of the northern and southern hemispheres. In the figure, the abscissa indicates the shift of the northern hemispheric rotational cycle length with respect to the southern hemispheric rotational cycle length, with negative values representing backward shifts. From the figure, one can find that the northern one lags the southern one by about 3 yr.

Figure 12 shows the cross-correlation coefficient between the rotational cycle length and the corresponding 2 yr smoothed daily hemispheric sunspot numbers. In the figure, the abscissa indicates the shift of the rotational cycle length with respect to the daily hemispheric sunspot numbers, with negative values representing backward shifts. From the figure, one can find that the rotational cycle length lags the sunspot numbers by about 1.8 yr in the whole disk, leads by about 190 d in the northern hemisphere, and lags by about 4.7 yr in the southern hemisphere. The three phase shifts are all different from one another, and the phase shifts in the whole Sun and in the northern hemisphere are both small, therefore the solar-cycle related variations of the rotational cycle length on the whole Sun and in the northern hemisphere look more similar to each other.

4 NORTH-SOUTH ASYMMETRY OF THE ROTATIONAL CYCLE LENGTH

4.1 North-South Asymmetry

The N-S asymmetry is traditionally calculated by means of formula $(N - S)/(N + S)$, where N and S stand for the rotational cycle length (or the 2 yr smoothed daily sunspot numbers) in the northern and southern hemispheres, respectively. The obtained values (the thin solid lines) and their
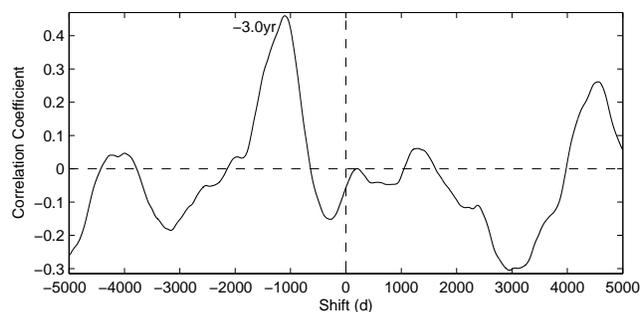
Fig. 11 Cross-correlation coefficient between the smoothed rotational cycle length of the northern and southern hemispheres, varying with the relative phase shifts between the two.
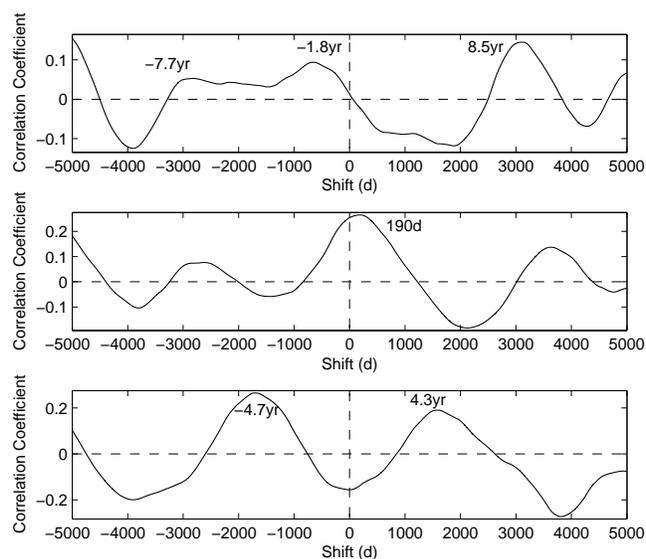
Fig. 12 The cross-correlation coefficient between the rotational cycle length and the corresponding 2 year smoothed daily hemispheric sunspot numbers. The three panels, from top to bottom, correspond to the whole disk, the northern hemisphere and the southern hemisphere.

regression lines (the thick dashed lines) are plotted in Figure 13. From the figure, one can find that the variation trend of the N-S asymmetry of the rotational cycle length displays the same variation trend as the N-S asymmetry of the daily sunspot numbers in the considered time interval. This means that in the considered time interval while solar activity in the southern hemisphere becomes stronger, the southern hemisphere rotates more slowly.

As Vizoso & Ballester (1990), Ataç & Özgüç (1996) and Li et al. (2002) did, here we fit a straight line to the daily values of the asymmetry for each of solar cycles 19 to 23 separately (cycles 18 and 24 are not a complete cycle in the considered time), starting each cycle with the time of the minimum between two consecutive cycles (see the thick solid lines in Fig. 13). The panels show that the slopes
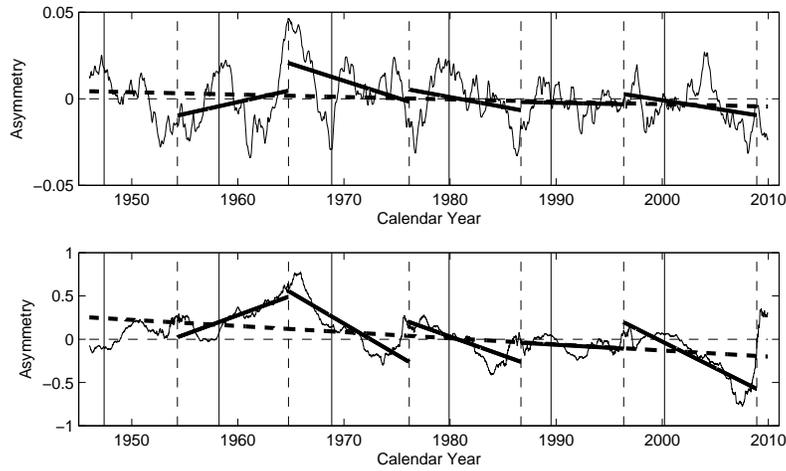
Fig. 13 Fit of a regression line to the daily value of the N-S asymmetry of the rotational cycle length (*top panel*) and that of the sunspot numbers (*bottom panel*) for solar cycles 19 to 23. The vertical solid (*dashed*) lines indicate the maximum (minimum) times of the sunspot cycles.

of these fitted straight lines are positive for the first cycle, but negative for the subsequent four cycles. Such a positive (negative) sign for a cycle here, in the top panel of Figure 13, means that the northern (southern) hemisphere rotates progressively more slowly, relative to the southern (northern) hemisphere, when solar activity is progressing in the cycle. A positive (negative) sign for a cycle in the bottom panel of Figure 13 means that the northern (southern) hemispheric solar activity becomes stronger, which is related to the southern (northern) hemispheric solar activity, when solar activity is progressing in the cycle. Comparing the two panels of Figure 13, we can conclude that, in a solar cycle, when one hemispheric solar activity becomes stronger, this hemisphere rotates more slowly. Vizoso & Ballester (1990) proposed a regularity that the slope of the straight fitted line changes its sign every four cycles, and there has been no exception so far. From the preceding discussion and the regularity condition, it is inferred that in cycle 24, the N-S asymmetry of the hemispheric PLRC should have a positive sign. At the beginning of cycle 24, the northern hemisphere thus should have a shorter rotational period. Also the northern hemisphere should rotate faster at first, and then more slowly.

Moreover, we investigate the periodicity of the N-S asymmetry of the daily hemispheric rotational cycle length by using the complex Morlet wavelet transformation again (Fig. 14), and find that no significant period (scale) seems to appear at the 11 yr Schwabe cycle, but there are two significant periods at the 95% confidence level, whose values are 7.7 and 17.5 yr (as the data are 2 yr smoothed, a 1.4 yr period is not reliable). The 7.7 yr period is much closer to the aforementioned period of the hemispheric rotational cycle length.

4.2 Relationship of the North-South Asymmetry of PLRC with that of Solar Activity

Figure 15 shows the cross-correlation coefficient between the N-S asymmetry of the rotational cycle length and the N-S asymmetry of the daily sunspot numbers. In the figure, the abscissa indicates the shift of the N-S asymmetry of the rotational cycle length with respect to the N-S asymmetry of the daily hemispheric sunspot numbers, with negative values representing backward shifts. As the figure shows, the two have a high correlation coefficient of 0.24 when there is no shift between the two.
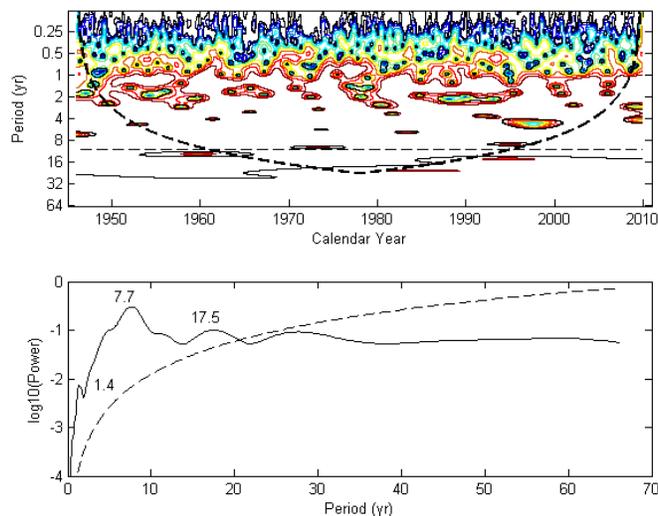
Fig. 14 *Top panel:* the continuous wavelet power spectrum of the N-S asymmetry of the rotational cycle length of the daily hemispheric sunspot numbers. The black solid contours indicate the 95% confidence level. The region below the thick dashed line indicates the COI where edge effects might distort the picture (Torrence & Compo 1998). The horizontal dashed line stands for the scale of 11.0 yr. *Bottom panel:* the global power spectrum (*solid line*) of the N-S asymmetry of the rotational cycle length of the daily hemispheric sunspot numbers. The dashed line shows the 95% confidence level.
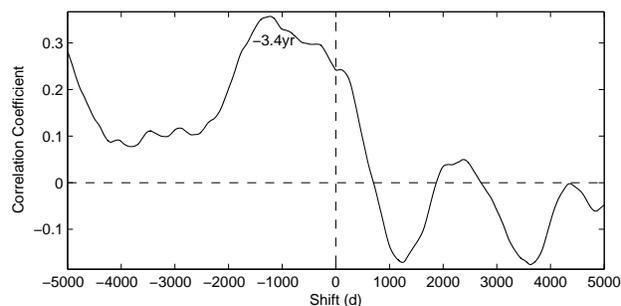
Fig. 15 Cross-correlation coefficient between the N-S asymmetry of the rotational cycle length and that of the daily hemispheric sunspot numbers, varying with the relative phase shifts between the two.

When the N-S asymmetry of the daily hemispheric sunspot numbers moves backwards by 3.4 yr, the cross-correlation coefficient reaches its peak.

5 CONCLUSIONS AND DISCUSSION

The long-term variations in solar rotation rate are studied in the northern and southern hemispheres, respectively, through a continuous wavelet transformation method from a global point of view, and the main results are listed as follows:

(1) The autocorrelation function indicates that the southern hemisphere rotates faster than the northern hemisphere in the considered time interval. Lustig (1983) studied the solar differential rotation by using the positions of sunspots in the years from 1947 to 1981, and found that the southern hemisphere had a smaller gradient of differential rotation than the northern hemisphere. In other words, the southern hemisphere rotated faster than the northern hemisphere. From table 1 of Javaraiah et al. (2005), we find that the southern hemisphere indeed has a smaller gradient of differential rotation. To answer the question of why the southern hemisphere rotates faster, one needs further study of the reasons for the difference in the long-term variations of the gradient of differential rotation in the two hemispheres.

(2) The rotational cycle length of the northern and southern hemispheres has different variation trends, but solar activity in the two hemispheres has the same variation trend. This means that the long-term variation trend of hemispheric rotation rate has no direct relation with the variation trend of solar activity in the considered time. Li et al. (2011c) pointed out that secular trends of solar rotation over an average of latitudes or at a certain latitude should change with latitude. Thus, it may be one possible reason for the different trends of the two hemispheres' rotational cycle length that the sunspots of the northern and southern hemispheres form in different average latitudes in the considered time. Further research is needed.

(3) The rotational cycle length of both hemispheres has no significant period (scale) appearing at the 11 yr Schwabe cycle, in accordance with Li et al. (2011a), but both have a significant period of about 7.6 yr, and this has been found in the periodicity of the surface equatorial rotation rate by Javaraiah et al. (2009).

(4) In the whole disk and the northern hemisphere, a higher than average velocity appears before the minimum time of solar activity. This may be caused by the phase difference and periodic difference between the hemispheric rotational cycle length and the hemispheric solar activity, and may also be influenced by the spatio-temporal distribution of the sunspots. The solar-cycle dependence of the two hemispheres' rotational cycle length is also different, and this may be the result of the phase shift between the northern and southern rotational cycle length, as well as the phase shift between the northern and southern solar activity.

(5) The rotational cycle lengths of the northern and southern hemispheres show a difference in their phases. Additionally, the phase shifts between the rotational cycle length and the sunspot numbers in the north, south and the whole disk are different from one another. Since the relation between the hemispheric rotation and the hemispheric sunspot activity is complex, in-depth research is needed.

(6) The N-S asymmetry of the rotational cycle length has the same variation trend as the N-S asymmetry of the solar activity in a solar cycle, as well as in the considered time interval. The N-S asymmetry of the rotational cycle length has two significant periods: 7.7 and 17.5 yr. Moreover, it has a high correlation with the N-S asymmetry of sunspot activity. On the basis of the aforementioned characteristics and the regularity advanced by Vizoso & Ballester (1990) and Li et al. (2002), it is inferred that the northern hemisphere should rotate faster at the beginning of solar cycle 24.

References

Antonucci, E., Hoeksema, J. T., & Scherrer, P. H. 1990, ApJ, 360, 296

Ataç, T., & Özgüç, A. 1996, Sol. Phys., 166, 201

Balthasar, H., Vazquez, M., & Woehl, H. 1986, A&A, 155, 87

Beck, J. G. 2000, Sol. Phys., 191, 47

Brajša, R., Ruždjak, D., & Wöhl, H. 2006, Sol. Phys., 237, 365

Carbonell, M., Oliver, R., & Ballester, J. L. 1993, A&A, 274, 497

Carbonell, M., Terradas, J., Oliver, R., & Ballester, J. L. 2007, A&A, 476, 951

Chowdhury, P., & Dwivedi, B. N. 2011, Sol. Phys., 270, 365

De Moortel, I., Munday, S. A., & Hood, A. W. 2004, Sol. Phys., 222, 203

Georgieva, K., & Kirov, B. 2003, in GONG+2002. Local and Global Helioseismology: the Present and Future, ed. H. Sawaya-Lacoste (ESA Special Publication), 517, 275

Gigolashvili, M. 2001, in Astronomische Gesellschaft Meeting Abstracts, 18, ed. E. R. Schielicke, 249

Gigolashvili, M. S., Mdzinarishvili, T. G., Japaridze, D. R., & Chargeishvili, B. B. 2003, New Astron., 8, 529

Gilman, P. A., & Howard, R. 1984, ApJ, 283, 385

Grinsted, A., Moore, J. C., & Jevrejeva, S. 2004, Nonlinear Processes in Geophysics, 11, 561

Heristchi, D., & Mouradian, Z. 2009, A&A, 497, 835

Howard, R. 1984, ARA&A, 22, 131

Howard, R., Gilman, P. I., & Gilman, P. A. 1984, ApJ, 283, 373

Javaraiah, J., Bertello, L., & Ulrich, R. K. 2005, ApJ, 626, 579

Javaraiah, J., & Ulrich, R. K. 2006, Sol. Phys., 237, 245

Javaraiah, J., Ulrich, R. K., Bertello, L., & Boyden, J. E. 2009, Sol. Phys., 257, 61

Lawrence, J. K., Cadavid, A. C., & Ruzmaikin, A. 2008, Sol. Phys., 252, 179

Le Mouël, J.-L., Shnirman, M. G., & Blanter, E. M. 2007, Sol. Phys., 246, 295

Li, K. J., Gao, P. X., & Qiu, J. 2006, ApJ, 646, 1392

Li, K.-J., Liang, H.-F., & Feng, W. 2010, RAA (Research in Astronomy and Astrophysics), 10, 1177

Li, K. J., Liang, H. F., Feng, W., & Zhan, L. S. 2011a, Ap&SS, 331, 441

Li, K. J., Shi, X. J., Liang, H. F., et al. 2011b, ApJ, 730, 49

Li, K. J., Feng, W., Shi, X. J., et al. 2011c, Sol. Phys. submitted

Li, K. J., Wang, J. X., Xiong, S. Y., et al. 2002, A&A, 383, 648

Li, K. J., Yun, H. S., & Gu, X. M. 2001, ApJ, 554, L115

Lustig, G. 1983, A&A, 125, 355

Paternò, L. 2010, Ap&SS, 328, 269

Schroeter, E. H. 1985, Sol. Phys., 100, 141

Snodgrass, H. B. 1992, in ASPC Series 27, The Solar Cycle, ed. K. L. Harvey, 205

Sýkora, J., & Rybák, J. 2010, Sol. Phys., 261, 321

Temmer, M., Rybák, J., Bendík, P., et al. 2006, A&A, 447, 735

Temmer, M., Veronig, A., & Hanslmeier, A. 2002a, in SOLMAG 2002. Proceedings of the Magnetic Coupling of the Solar Atmosphere Euroconference, ed. H. Sawaya-Lacoste (ESA Special Publication), 505, 587

Temmer, M., Veronig, A., & Hanslmeier, A. 2002b, A&A, 390, 707

Temmer, M., Veronig, A., Rybák, J., & Hanslmeier, A. 2003, Hvar Observatory Bulletin, 27, 59

Torrence, C., & Compo, G. P. 1998, Bulletin of the American Meteorological Society, 79, 61

Verma, V. K. 1993, ApJ, 403, 797

Vizoso, G., & Ballester, J. L. 1990, A&A, 229, 540

Yin, Z.-Q., Han, Y.-B., Ma, L.-H., Le, G.-M., & Han, Y.-G. 2007, ChJAA (Chin. J. Astron. Astrophys.), 7, 823

Zuccarello, F., & Zappalá, R. A. 2003, Astronomische Nachrichten, 324, 464